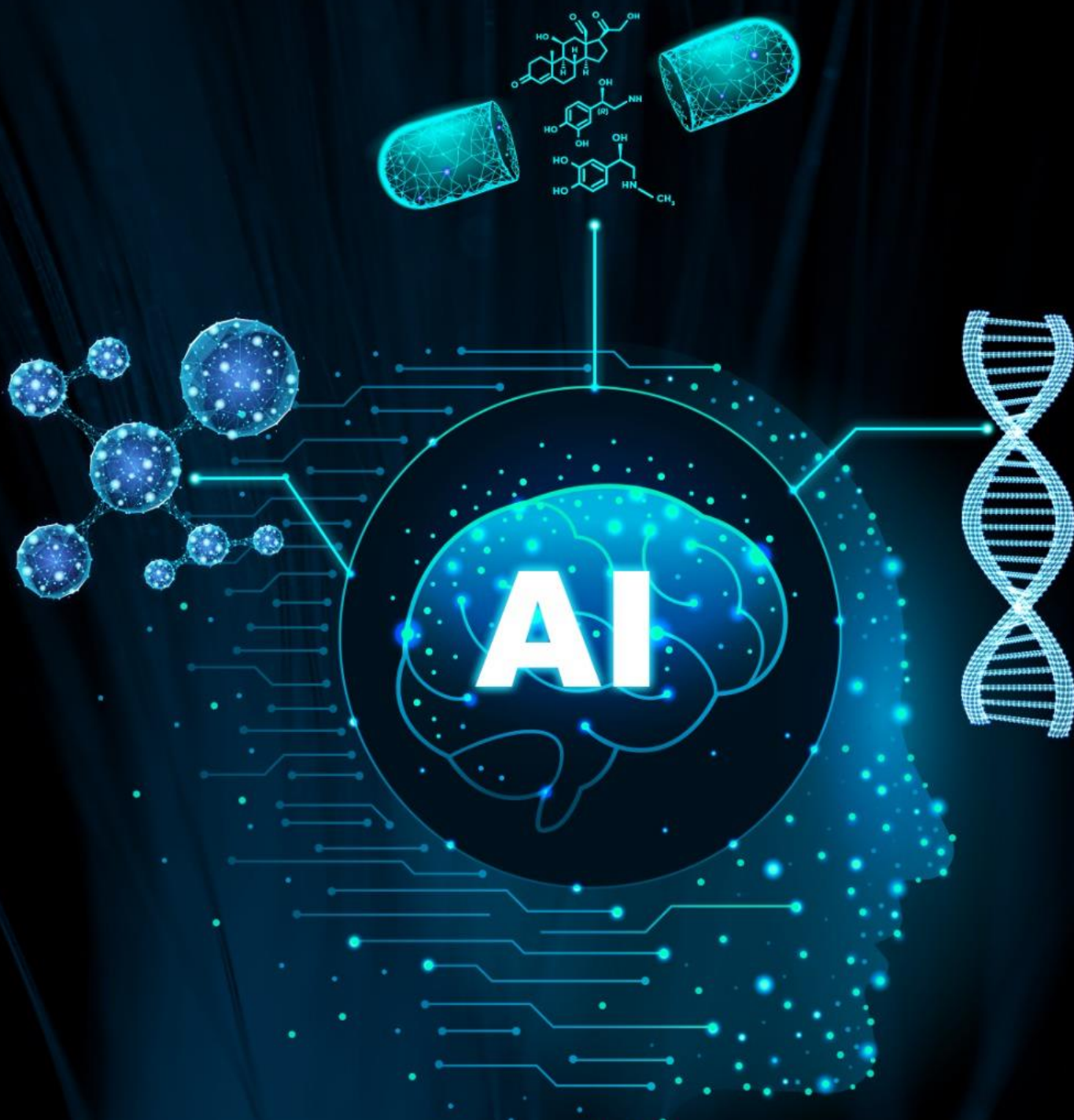


# CYBER AIDD

## WEEKLY REPORT



# Cyber-AIDD Screening of series of orally available androgen receptor degraders for the treatment of prostate cancer

(Reference from Journal of medicinal Chemistry-2024,67,14,11732-11750)

## Part 1

Androgen receptor (AR) signaling plays an important role in the progression of prostate cancer. The paper reported a New AR Discovery and optimization of PROTAC degraders. AR based on 4-(4-phenyl-1-piperidiny)-2-(trifluoromethyl) benzonitrile small molecules. After ligand That PROTAC optimization strategies focus on linker connectivity and CRBN ligands of SAR Research, to achieve effective degradation of AR in LNCaP cells. Found Compounds 11 and 16 showed good oral bioavailability. The study found Another ideal feature, i.e., degradation of the important therapeutic resistance mutation L702H. Compound 22 (AZ'3137) right AR and L702H mutant AR have degradation effect, and has good oral bioavailability across species. The compound also inhibits AR signaling in vitro and tumor growth in vivo in a mouse prostate cancer xenograft model.

Pharmacodia CyberSAR system provides in-depth analysis of AR target molecules. The system displays active molecules related to the target through clustered structure views and original structure views, and presents potential hits in the form of a timeline during the R&D stage. In addition, CyberSAR also provides visual analysis of indications and experimental designs to help R&D personnel quickly obtain target structure information and open up research ideas. Although CyberSAR has not been used in the initial development of molecules, it shows great application potential in analyzing and optimizing drug molecules.

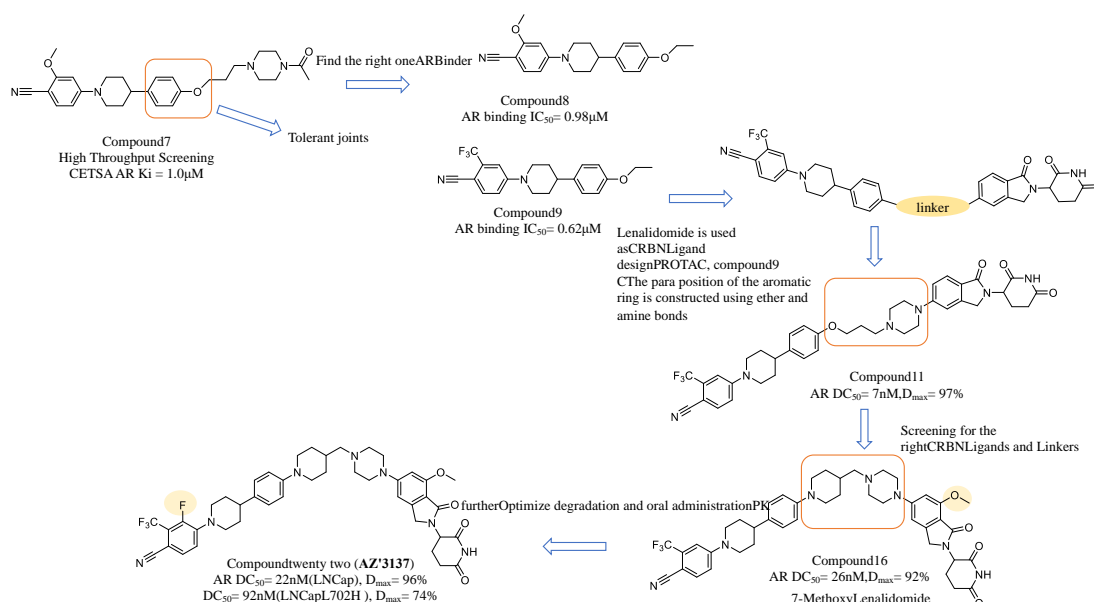


Figure 1. AZ'3137 Discovery and molecule optimization process

ARTICLE | July 11, 2024

**Discovery of a Series of Orally Bioavailable Androgen Receptor Degraders for the Treatment of Prostate Cancer**

Sharan K. Bagal\*, Peter C. Asfles\*, Cours Diéne, Argirides Argyros, Claire Crafter, Doyle J. Casar, Charlene Fallon, Andreas Hoek, Thomas Jones, Kevin Moreau, Gillian M. Lamont, Scott Lamont, Chrysis Michalogiorgou, Martin J. Packer, Andy Pike, Antonio Ramos-Montoya, James S. Scott, Joseph Shaw, and Ziyanda Sholaja



Journal of Medicinal Chemistry  
Cite this: *J. Med. Chem.* 2024, 67, 14, 11732–11750  
<https://doi.org/10.1021/acs.jmedchem.4c00269>  
Published July 11, 2024  
Copyright © 2024 American Chemical Society  
Request reuse permissions

## Part 2

Traditional small molecule drugs bind to target proteins as a way to modulate specific biological activities. In contrast, proteolysis targeting chimeric molecules (PROTACs) bind to their target proteins and subsequently cause their degradation. Unlike traditional small molecule occupancy-driven inhibitors or antagonists, PROTAC-driven protein degradation can theoretically produce more profound biological responses that extend beyond the pharmacokinetic half-life of the molecule (which instead depends on the resynthesis rate of the protein).

PROTAC molecules can be divided into three parts, the first part is able to bind to the target protein (POI) to be degraded, the second part is able to bind to the E3 ubiquitin ligase and the linker connecting these two parts. POI degradation occurs when PROTAC binds to the target protein and E3 ubiquitin ligase simultaneously into a quaternary complex. The E3 ligase then recruits the E2 conjugating enzyme into the ternary complex, thereby ubiquitinating the target protein. This has the effect of marking the target protein for recognition/degradation by the cellular proteasome machinery. PROTAC can then dissociate from the target protein and initiate another cycle of this degradation process, driving its degradation with lower target occupancy. The androgen receptor (AR) belongs to the nuclear receptor steroid hormones and is a ligand-dependent transcription factor that controls the expression of a series of genes involved in prostate cell growth and survival. The AR is composed of four distinct domains: the N-terminal domain (NTD), the DNA binding domain (DBD), the hinge region that allows the N-terminus and C-terminus to interact, and the C-terminal ligand binding domain (LBD). Androgens such as testosterone and its derivative dihydrotestosterone (DHT) bind to the AR ligand binding domain, releasing AR partner proteins, allowing AR to dimerize and translocate from the cytoplasm to the nucleus. Within the nucleus, AR dimers bind to androgen response elements (AREs) in the promoters of androgen-responsive genes, such as KLK3 (prostate-specific antigen, PSA) and FKBP5. The AR signaling pathway is essential for normal prostate development, and male sexual differentiation does not occur without androgens or without functional AR.

The relationship between AR signaling and prostate cancer was first discovered by Huggins and Hodges in 1941 in semen studies, and subsequent studies have shown that androgen deprivation therapy is very effective in treating recurrent prostate cancer. However, despite initial response, most tumors adapt to low androgen levels, and patients relapse within a few years and develop a disease state called castration-resistant prostate cancer (CRPC). Several antiandrogens have been approved for the treatment of CRPC, including the nonsteroidal AR antagonists bicalutamide, enzalutamide, and apalutamide (Figure 1) and the androgen biosynthesis inhibitor abiraterone. AR antagonists compete with androgens for

binding to the steroid LBD, inhibiting nuclear translocation and DNA binding, thereby effectively shutting down AR signaling. In contrast, the androgen biosynthesis inhibitor abiraterone targets the cytochrome P450 enzyme CYP17A1 and reduces the formation of the androgens DHEA and androstenedione (precursors of testosterone and DHT), thereby reducing AR excitation and inhibiting prostate tumor growth.

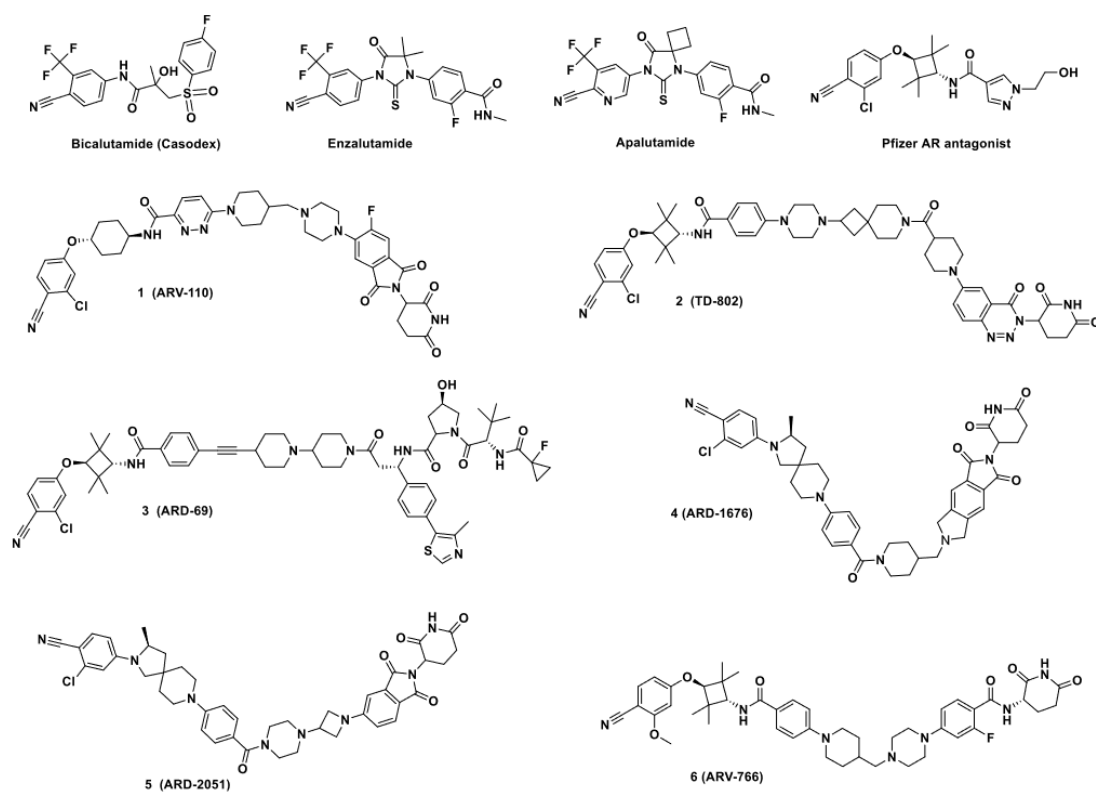


Figure 1. AR antagonists and AR PROTAC degraders.

Although the above drugs have significantly prolonged the survival of patients with advanced prostate cancer, resistance inevitably occurs. Several mechanisms of resistance have been identified, including AR amplification, point mutations, or the generation of splice variants lacking the ligand binding domain. Specific AR mutations (L702H, W742L/C, H875Y, F877L, and T878A/S) have been found in up to 20% of prostate cancer patients after the emergence of treatment resistance. These ligand binding site mutations change the binding affinity of ligands (including steroids and antiandrogens) and lead to altered responses to AR pathway inhibitors, for example, converting antagonists to agonists or allowing the receptor to utilize alternative steroid hormones such as glucocorticoids or progesterone. L702H is located at the exit of the AR steroid binding pocket and is a highly common point mutation that occurs in approximately 10% of patients as a single or concurrent mutation, enabling glucocorticoids to agonize AR. Therefore, drugs that degrade AR and thereby remove it from cells could overcome LBD resistance and, in addition to improving efficacy, may provide enhanced therapeutic benefit for patients with advanced, refractory prostate cancer.

A key step toward testing this hypothesis in the clinic was the discovery of ARV-110, bafoderglutamine (1), by scientists at Arvinas. This compound is the first orally

bioavailable AR PROTAC degrader to enter clinical studies. Preclinical data showed that ARV-110 is a potent AR degrader that reduces protein levels and inhibits cell proliferation in relevant prostate cancer cells at low nM concentrations. ARV-110 is an orally available therapeutic that maintains efficacy in rodent prostate cancer xenograft models in the absence of AR antagonists such as enzalutamide. Recent clinical data showed that ARV-110 is well tolerated in patients and demonstrated that it can reduce AR levels in tumors and PSA levels in plasma, a key marker for prostate cancer. Several other AR PROTACs have now been published in the literature, using VHL and CRBN recruiting ligands as E3 ligands, and many have shown good oral bioavailability and efficacy in prostate cancer models. Figure 1 shows some molecules, including TD80219 (2) and ARD-69 (3), which are based on Pfizer's published tetramethylcyclobutylARBinding motif as ARAntagonists and **ARD-1676 (4)** and **ARD205124 (5)**, which includes the new ARBinding ligand. In addition to ARV-110, several AR PROTACs have entered clinical development, including ARV76626 (luxdegalutamide) ( 6 ) , CC-94676/AR-LDD (BMS/ Celgene), JMKX002992 (Roche/ Shanghai Jimin Kexin) and AC-0176 (Accutar). Recent advances in clinical development (6) have highlighted treatment options for heavily pretreated patients, including those with the AR L702H mutation.

This article reports the discovery of a series of new potent AR ligands and their development into orally bioavailable PROTAC degraders. Notably, the use of E3 ligands for CRBN facilitates the oral bioavailability of PROTACs. To date, these ligand-derived IMiD-class CRBN modulators lenalidomide and pomalidomide (e.g., 1, 4, 5) or variants of these ligands (e.g., 2, 6), and more novel CRBN ligands are under development.

### **AR Binding molecule ligand choose**

AstraZeneca has a wealth of targeted AR Antagonists Bicalutamide Development Experience, which is the first generation of nonsteroidal AR antagonists, in 1982 get patent Authorization, approved in 1995 for the treatment of prostate cancer. After discovery AstraZeneca has also discovered several other AR-targeting small molecules that have also entered clinical trials. Small molecules, you can choose from Therefore, a meta-analysis of AR binding data was performed and 20,000 compounds were ultimately selected for human AR Rescreening in binding assays. As an initial sorting of the actives in this screen, 100 compounds from this group were prioritized for screening in a high-throughput cellular thermal shift assay (CETSA). This CETSA assay was developed in-house Methods, aimed to determine intracellular target binding of AR using the disease-relevant LNCaP cell line. The preliminary data set provided an interesting result, compound 7, which had a CETSA binding  $K_i$  of 1.0  $\mu\text{M}$  (Figure 2). Based on this result, truncated compounds 8 and 9 were synthesized and discovered for Powerful AR Binder, Determination Its AR Ligand Binding domain active  $\text{IC}_{50} < 1.0 \mu\text{M}$  Compound 8 and 9 It is a small molecular weight but high ligand efficiency (MW <400, ligand efficiency=0.32–0.34), relatively rigid (low number of rotatable bonds), and lacking hydrogen bond donors (HBD) neutral molecules. From producing orally bioavailable PROTAC In addition, the lead

compound molecules **7** show C The para position of the cycloaryl group can tolerate the linker and thus will be the construction PROTACA suitable carrier.

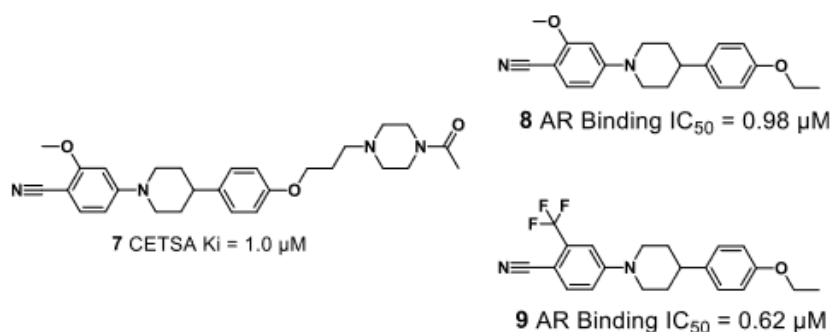
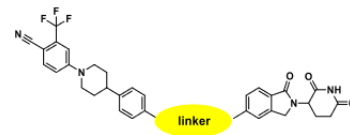


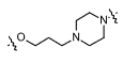
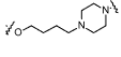
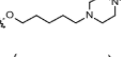
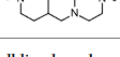
**Figure 2.** AR binding hit from AstraZeneca collection and truncated derivatives.

### PROTAC Design

All DC50 data are presented using geometric mean values. Dmax values represent the maximum degradation observed relative to the DMSO control (set to 0% degradation) and the 3  $\mu\text{M}$  literature reported AR PROTAC control (set to 100% degradation). Notably, analysis of AR binding compounds **8** and **9** showed minimal activity in this assay (<50% effect at 10  $\mu\text{M}$ ). Compound **9** with a CF<sub>3</sub> substituent was first selected for PROTAC assembly based on its binding potency to AR (Figure 2). Table 1 presents the PROTACs generated by constructing the para position of the C ring aromatic group **9** using ether and amine bonds. Using lenalidomide as a CRBN binder and applying the piperazine 3-carbon chain ether linker to the AR binder resulted in PROTAC **10**. This PROTAC was an effective AR degrader in the LNCaP cell line (DC50 = 16 nM, Dmax = 79% for **10**). Increasing the ether chain length to 4- and 5-carbons resulted in PROTACs **11** and **12**, respectively. The maximum degradation (Dmax) observed after modification increased to >90% while maintaining potency (**11** DC50 = 7 nM, Dmax = 97%, **12** DC50 = 15 nM, Dmax = 94%). Replacing the ether chain in the linker with piperidine maintained the potency of **13**, although the maximum degradation was slightly reduced (DC50 = 18nM,Dmax=85%), which indicates that the introduction of a flexible linker is advantageous. As a preliminary assessment of the physicochemical properties and pharmacokinetics, PROTAC In the lipophilicity determination (Chrom Log-D) In vitro human microsomal internal clearance (CLint) Determination (HuMics, surface1) were analyzed. PROTAC **10–13**Is lipophilic (Chrom Log-D > 5), with low to moderate measurable CLint (HuMics <15  $\mu\text{L}/\text{min}/\text{mg}$ ). PROTAC **11** Possessing good potency, maximum degradability, lipophilicity and in vitro CLint the indices were balanced and thus became the key analogs for further analysis.

Table 1. Linker SAR of AR PROTACs

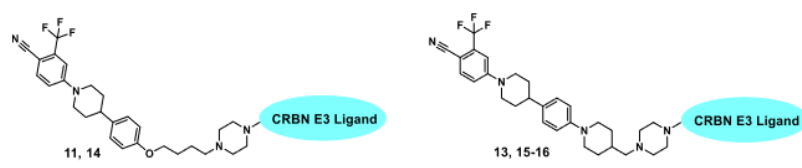


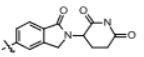
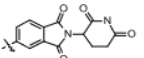
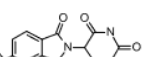
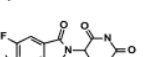
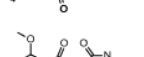
Compound	LINKER	AR degradation		ChromLogD <sup>c</sup>	Hu Mics ( $\mu\text{L}/\text{min}/\text{mg}$ ) <sup>d</sup>
		DC <sub>50</sub> (nM)	Dmax (%) <sup>a,b</sup>		
10		16	79	5.2	5
11		7	97	5.4	10
12		15	94	5.6	12
13		18	85	5.9	3

<sup>a</sup>Mean AR degradation in the LnCAP cell line based on  $n \geq 2$ . <sup>b</sup>0% control is DMSO and 100% AR degrader control at 3  $\mu\text{M}$  is VHL PROTAC N-[(5-[(4-[(1*r*,3*r*)-3-(3-chloro-4-cyanophenoxy)-2,2,4,4-tetramethylcyclobutyl]carbamoyl]phenyl)amino]pentyl]oxy)acetyl]-3-methylvalyl-(4*R*)-4-hydroxy-N-[(1*S*)-1-[4-(4-methyl-1,3-thiazol-5-yl)phenyl]ethyl]-1-prolinamide (WO2016118666). <sup>c</sup>ChromLogD compound lipophilicity using the retention on a C18 chromatographic stationary phase in a reverse-phase ultrahigh-performance liquid chromatography (HPLC/UPLC) system at pH 7.4. <sup>d</sup>Intrinsic clearance in human liver microsomes ( $\mu\text{L}/\text{min}/\text{mg}$ ) determined from DMSO stock solutions.

Using PROTACs 11 and 13 (Table 1) as a starting point, we altered CRBNBinderTo further optimize the degradationactiveand properties (Table 2). A pomalidomide analogue of PROTAC 11 was synthesized as 14. PROTAC14 was three times less potent than 11 and had a higher lipophilicity andClearanceShows that it is worse than 11 (14 DC50=22nM, Dmax=100%, ChromLogD=6.2, HuMics=21 $\mu\text{L}/\text{min}/\text{mg}$ ). PROTAC 15–16 is paired with PROTAC 13, where 15by6-FluoropomalidomideAsCRBNBinder, which is the first in ARV-110Used(Figure 1).and 16 to introduce 7-methoxylenalidomide groupsSex ratio,156-Fluoropomalidomide in the 13-mg/mL sham-treated mice did not offer any potency advantage and was in fact 10-fold less potent than 13 (13 DC50=18 nM, Dmax= 85% vs. 15DC50=180nM, Dmax= 92%), while the 7-methoxylenalidomide group in 16 remained similar to that in 13active(16 DC50=26nM, Dmax=92% vs.13DC50=18 nM, Dmax= 85%). The human liver microsomal clearance in these two groups was very low (<3 $\mu\text{L}/\text{min}/\text{mg}$ ), but this makes them attractivenature,includeSubsequent PROTAC Design. In the course of this work, other groups in the field have reported on the utility of 7-methoxy substitutions in influencing CRBN neosubstrate selectivity. Here, the authors confirmed that 11 resulted in SALL4 degradation, whereas the 7-methoxy derivative 16 did not (Supplementary Fig. S1). In addition to IMiD neosubstrates, reduced binding of 16 to cardiovascular-relevant voltage-gated L-type calcium channels compared with 11 was observed (Supplementary Table S3), suggesting that the 7-methoxy derivative may provide additional effects beyond reduced IMiD neosubstrate degradation.

**Table 2. CRBN Binder SAR of AR PROTACs<sup>a</sup>**



Compound	E3	AR degradation		ChromLogD <sup>c</sup>	Hu Mics ( $\mu\text{L}/\text{min}/\text{mg}$ ) <sup>d</sup>
		DC <sub>50</sub> (nM)	Dmax (%) <sup>a,b</sup>		
11		7	97	5.4	10
14		22	100	6.2	21
13		18	85	5.9	3
15		180	92	7.0	<3
16		26	92	5.7	<3

<sup>a,b,c,d</sup>Details as for Table 1.

### Pharmacokinetic characteristics of AR PROTACs

The exposed polar surface area (ePSA) measured for PROTACs 11 and 16 (Table 1) is 121 Å<sup>2</sup> and 126 Å<sup>2</sup>, which is in the range that might be expected to have measurable oral bioavailability in rodents. PROTAC 11 and 16 pharmacokinetic studies were subsequently performed in mice, rats, and dogs (Table 3). Compound 11 and 16 low to moderate clearance was observed in all species with moderate to high distribution. 5:95 DMSO:Sulfobutyl ether- $\beta$ -Cyclodextrin (30% w/v) when the solution is administered, the oral bioavailability in rodents is  $\geq 20\%$ . This shows that although 11 and 16 exist, Caco-2 permeability in the cell lines was significantly poorer ( $P_{app} < 0.05 \times 10^{-6}$  cm/s) and in pH 7.4 poor water solubility in buffer (<2  $\mu\text{M}$ ), but it has a moderate absorption potential. However, 11 and 16 the oral bioavailability of <20%, indicating that there is still some absorption risk.

**Table 3. In Vivo Pharmacokinetics of Compounds 11, 16 and 22<sup>a</sup>**

species	11			16			22		
	mouse <sup>b</sup>	rat <sup>c</sup>	dog <sup>d</sup>	mouse	rat	dog	mouse	rat	dog
CL (mL/min/kg)	16	15	4.0	4.4	11	8.1	2.0	7.4	3.0
Vss (L/kg)	5.2	6.2	7.1	2.4	7.8	13	1.5	9.0	2.4
T1/2 (h)	5.0	6.6	53.5	6.8	9.1	21	9.0	11	12.5
oral F (%)	47	20	8	50	27	19	62	29	18

<sup>a</sup>All studies are  $n = 2$ . <sup>b</sup>CD-1 mouse following 0.5 mg/kg i.v. bolus and 1 mg/kg p.o. formulated in 5% DMSO/95% 30% w/v sulfobutylether- $\beta$ -cyclodextrin. pH adjusted as required to a range of 3–6 to obtain a solution. <sup>c</sup>Han Wistar rat following 0.5 mg/kg i.v. bolus and 1 mg/kg p.o. formulated in 5% DMSO/95% 30% w/v sulfobutylether- $\beta$ -cyclodextrin. pH adjusted as required to a range of 3–6 to obtain a solution. <sup>d</sup>Beagle dogs following 0.5 (compound 16 = 0.2) mg/kg i.v. infusion over 0.25 h and 1 mg/kg p.o. formulated in 5% DMSO/95% 30% w/v sulfobutylether- $\beta$ -cyclodextrin. pH adjusted as required to range of 3–6 to obtain a solution.

Based on the promise of compounds 11 and 16, the SAR around the AR binding region of these molecules was explored to assess whether degradation potency and oral PK could be further optimized. As it was expected that the steroid ligand binding site might not accommodate large substituents, these studies were focused on F atom

modifications (Table 4). Another parameter that was desired to be measured was the potency of PROTACs to degrade the L702H mutation of AR. As discussed above, the ability of AR degraders to overcome this common mechanism of therapeutic resistance may provide an advantage to patients.

Table 4. AR Binding Region SAR of AR PROTACS

cmpd	R <sup>1</sup>	R <sup>2</sup>	R <sup>3</sup>	R <sup>4</sup>	R <sup>5</sup>	X	AR degradationDC <sub>50</sub> (nM)/D <sub>max</sub> (%) <sup>a,c</sup>	AR (L702H) degradationDC <sub>50</sub> (nM)/D <sub>max</sub> (%) <sup>b</sup>	mouse oral PK <sup>c</sup> CL (mL/min/kg)/V <sub>ss</sub> (L/kg)/T <sub>1/2</sub> (h)/F (%)
13	H	H	H	H	H	CH <sub>2</sub>	18/85	>3000/-	3.0/4.5/19/46
17	F	H	H	H	H	CH <sub>2</sub>	23/95	77/65	1.3/2.0/19.5/48
18	CH <sub>3</sub>	H	H	H	H	CH <sub>2</sub>	152/70	>3000/-	
19	Cl	H	H	H	H	CH <sub>2</sub>	48/80	144/79	
20	F	H	H	H	H	C=O	170/100	1330/100	2.5/6.2/32/77
21	F	H	H	F	H	C=O	87/100	992/100	
16	H	H	H	H	OCH <sub>3</sub>	CH <sub>2</sub>	26/92	>3000/-	4.4/2.4/6.8/50
22	F	H	H	H	OCH <sub>3</sub>	CH <sub>2</sub>	22/96	92/74	2.0/1.5/9.0/62
23	F	F	H	H	OCH <sub>3</sub>	CH <sub>2</sub>	12/100	469/100	1.6/2.2/17/50
24	F	F	F	H	OCH <sub>3</sub>	CH <sub>2</sub>	18/100	633/80	1.2/3.6/41/30
11	H						7.0/97	>3000/-	16/5.2/5.0/47
25	F						9.0/100	107/78	7.5/3.4/7.0/30

<sup>a</sup>Details as for Table 1. <sup>b</sup>Mean AR degradation in L702H mutant LNCAP cell line based on  $n \geq 2$ . <sup>c</sup>Compounds in PK studies were coadministered as mixtures of  $\leq 5$  compounds at 0.5 mg/kg/compound i.v. and 1 mg/kg/compound p.o. in 5% DMSO:95% hydroxypropyl- $\beta$ -cyclodextrin (30% w/v) at a volume of 2 and 4 mL/kg respectively.

The first observation is that compounds 11 and 16 as well as ARV-110 (1) are potent degraders of AR but do not degrade the L702H mutant of AR (1, **11**, **16** AR L702H > 3000 nM). The second striking observation is that the four PROTACoff in benzonitrile ring Atomic Introduction of R1 sustained AR degradation and resulted in degradation of the AR(L702H) mutant. The N-linked piperidine ring ortho-position F was observed in several matching pairs (13 and 17, 16 and 22, and 11 and 25). atom Since there is no protein ligand, X-ray Crystal structure, the reason for this observation is unclear. author It was hypothesized that the conformational effect of the ortho-F on the piperidine and subsequent rings could be combined with mutations in the LBD. To further explore this effect, larger methyl and chloro substituents were observed at R1 (18 and 19, respectively), but the potency of AR and AR (L702H) was lost compared to compound 17. Ortho-F atoms were also introduced at R2 and R3 of the phenyl ring (23, 24), which maintained the degradation potency of AR, but interestingly lost potency in the L702H mutant. Degradation potency. Compared to matched pair compound 22. As seen previously, the use of pomalidomide as an E3 recruiting ligand (20 and 21) resulted in a loss of potency for both AR and AR(L702H). In general, all compounds in Table 4 exhibited good mouse oral bioavailability >30%, with the more rigid piperidine-methylene-piperazine linker being the most potent. Compound 22 had the best overall profile, showing degradation DC50s <100 nM for both AR and AR(L702H) and good mouse oral bioavailability of 62%. Cross-species PK of the 22 compounds showed moderate oral bioavailability in rats (29%) and dogs (18%) (Table 3), and the compound had very low human liver microsomal clearance (<3  $\mu$ L/min/mg). Based on these data,

compound 22 (hereafter referred to as AZ'3137) was selected for further in vitro and in vivo characterization.

First, the authors utilized an AR imaging assay to confirm AR degradation in LNCaP cells endogenously expressing AR T878A and compared it to ARV110, a clinical AR PROTAC. Both compounds caused effective degradation of AR (Figure 3A). However, when evaluating degradation in CRISPR-edited LNCaP cells expressing AR T878A/L702H (LNCaP L702H), AZ'3137 was still able to degrade AR, while ARV-110 was inactive (Figure 3B). The results for ARV110 are consistent with preclinical assay data published by Arvinas and with previously identified patients who were treated with novel hormonal agents (NHAs) and were found to carry AR.L702H in order to further explore AZ'3137 degradation in AR-exposed C4-2 cells, androgen-independent LqCySubfamily and VCAP cells, wild-type expressing amplified AR of androgen-sensitive prostate cancer cell lines to increase AZ'3137 or ARV-110 The concentration of AR level. AZ'3137 Able to degrade C4-2 cells (Fig.3C) and VCAP cells (Fig.3D) AR, its effectiveness and Dmax and ARV-110 resemblance

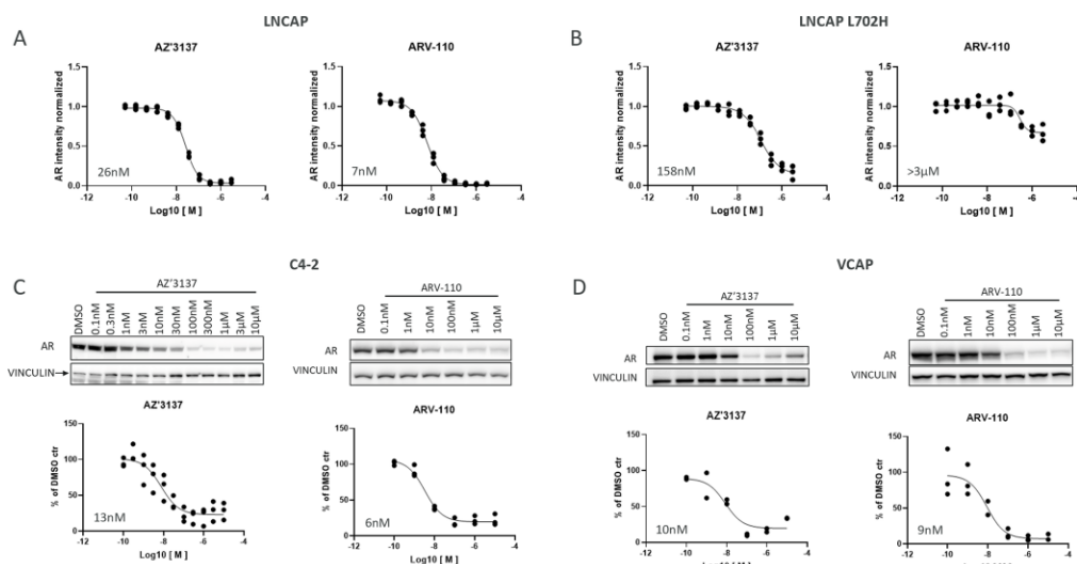


**Figure 3.** AZ'3137 degrades amplified and mutant AR. (A, B) Imaging of nuclear AR levels in (A) LNCaP cells and (B) LNCaP L702H cells, treated with increasing concentrations of AZ'3137 or ARV-110 for 24 h, using the IF assay. Raw data were normalized to mean total intensity observed in single-agent control wells. Data points from three independent experiments are shown. (C, D) Western blot analysis of C4-2 cells (C) and VCAP cells (D) treated with increasing concentrations of AZ'3137 or ARV-110 for 24 h and probed for AR and vinculin. Upper panels show a representative immunoblot for each cell line and compound. Lower panels represent the quantified data, relative to DMSO control, from 2 to 3 separate experiments. Mean DC<sub>50</sub> values are displayed in the bottom left corner of each plot.

Next, the authors tested the ability of AZ'3137 to inhibit AR transcriptional activity by measuring gene expression levels of six AR target genes. It was found that AZ'3137 was able to inhibit the expression of AR target genes in LNCaP cells with similar potency and to a similar extent as enzalutamide (Figure 4A). AZ'3137 had no effect on AR mRNA levels, which is consistent with AZ'3137 acting as an AR degrader rather than an AR synthesis inhibitor (Supporting Information, Figure S2). In addition, AZ'3137 inhibited the proliferation of LNCaP with a GI50 value of 74nM, which is equivalent to or better than the three AR antagonists enzalutamide, apalutamide, and darolutamide (Figure 4B). Together, these data indicate that AZ'3137 is a potent AR degrader that inhibits AR signaling and proliferation to a similar extent as clinical AR

antagonists.

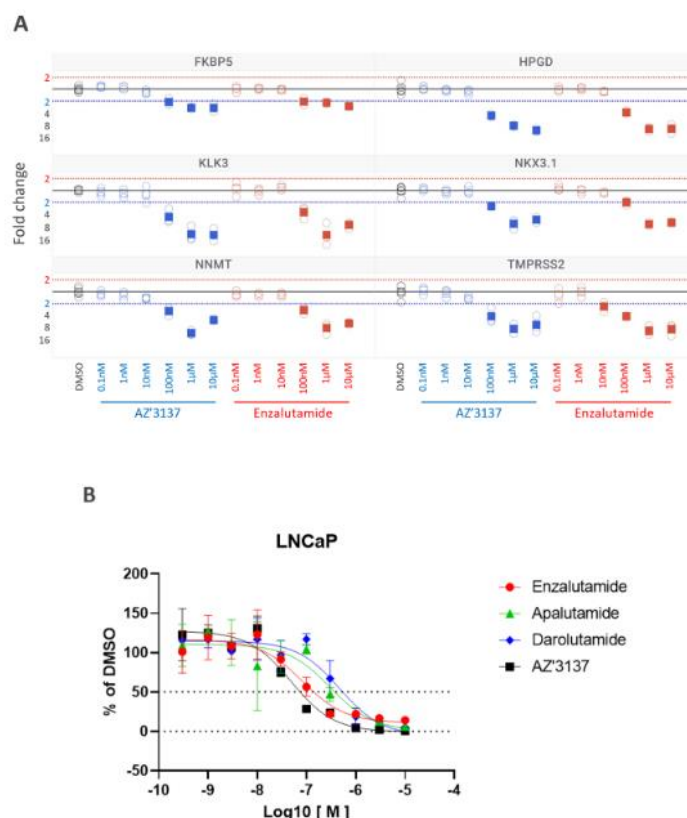


**Figure 4.** AZ'3137 inhibits AR signaling and cell growth in vitro (A) LNCaP cells were treated with enzalutamide or AZ'3137 for 24 h and expression levels of 6 genes were measured by QRT-PCR. NegddCt data were calculated for all 6 genes and plotted here as individual data (open circles) and mean data (open and filled squares). Open squares represent mean data with a  $p > 0.05$  and filled squares represent mean data with  $p < 0.05$  and are considered statistically significant. (B) 7-day proliferation assay of LNCaP cells treated with AZ'3137 or AR antagonists.

To explore the mechanism of AR degradation, author AZ'3137 was tested for its ability to degrade AR in the presence of excess lenalidomide (CRBN ligand) and excess enzalutamide (a potent AR binder). In both cases, the extent and potency of AR degradation were severely affected (Figure 5). Furthermore, the addition of the proteasome inhibitor MG132 completely blocked AR degradation. Altogether, these data confirm that AZ'3137 degrades AR via a PROTAC-induced mechanism that requires simultaneous binding of AR and CRBN and proteasome activity. Any mechanism occurs (Significant 5), as evidenced by (i) the lack of AR degradation when CRBN could no longer be recruited, i.e., in the presence of lenalidomide (FIG 5) and (ii) the minimal degradation activity observed with PO ligands 8 and 9 (<50% activity at 10  $\mu$ M).

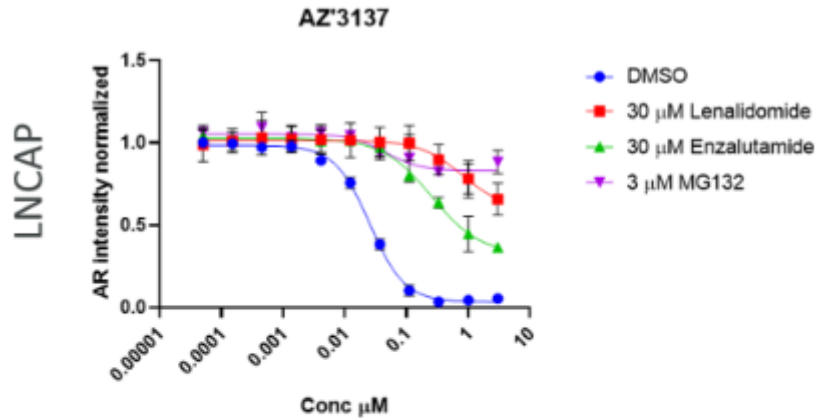


**Figure 5.** Confirmation of the PROTAC mechanism of action for AZ'3137 in LNCaP cells. Imaging of nuclear AR levels using IF assay. Raw data normalized to mean total intensity observed in single-agent control wells for each condition (ie., DMSO only, lenalidomide only, enzalutamide only and MG132 only) then analyzed in Graphpad Prism as a nonlinear four parameter fit.  $N = 3$  data exhibited as mean  $\pm$  SD. NB, the data for DMSO are the same as plotted in Figure 3A.

The author in vivo use of C4-2 in mice cell xenografts were used to test the ability of oral AZ'3137 to inhibit AR-dependent tumor growth in vivo. When tested in a pharmacodynamic (PD) study, AZ'3137 achieved greater than 90% AR degradation at 30 mg/kg (Figure 6A). The final total plasma concentration of AZ'3137 was  $\sim$ 20  $\mu$ M at the end of the study. Due to the challenging nature of this compound, accurate values for the unbound fraction in mouse plasma could not be obtained. AZ'3137 was shown to be well tolerated in mice (Supplementary Figure S3) and plasma exposure could be achieved, resulting in excellent AR degradation in vivo. Next, its activity at C4-2 cell antitumor activity in 28At the end of the 4-day dosing period, AZ'3137 resulted in 70% inhibition of tumor growth, which is comparable to the effect achieved by 50 mg/kg of enzalutamide and 10 mg/kg, a clinically relevant dose of ARV-110 (FIG. 6B).

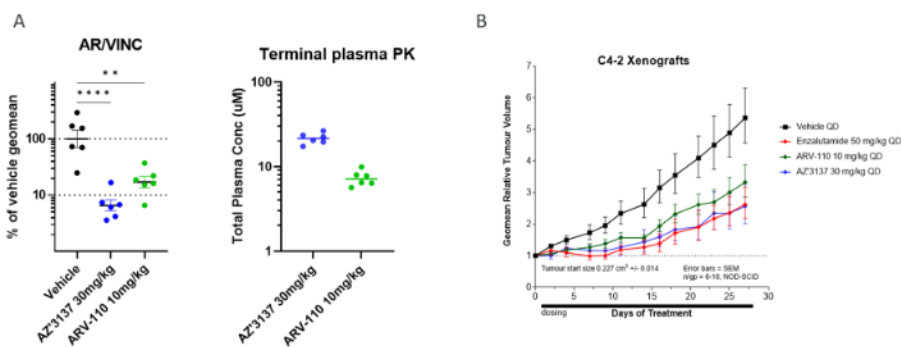


**Figure 6.** AZ'3137 degrades AR and inhibits tumor growth in vivo. (A) Left panel: AR protein levels in C4-2 tumor samples treated with vehicle, AZ'3137 at 30 mg/kg or ARV-110 at 10 mg/kg for 10 days. Individual vinculin-corrected values are plotted ( $n = 6$ ) with mean  $\pm$  SEM shown. Right panel: total compound concentrations in terminal plasma samples collected 6 h after last dose (day 10;  $n = 6$ , mean). (B) Antitumor activity of 30 mg/kg AZ'3137, 50 mg/kg enzalutamide, or 10 mg/kg ARV-110 in the C4-2 xenograft tumor model in SCID mice. Compounds and vehicle control were dosed orally once daily for 28 days.

### In conclusion

This article reports the discovery and optimization of a series of androgen receptor PROTAC degraders for the treatment of prostate cancer. Screening

compounds 1-(4-Cyanophenyl)-4-arylpiperidines (e.g., compounds 8, 9) were selected as novel AR-binding ligands. SAR studies identified the optimal linker and E3 ligase-binding ligands for CRBN to develop these AR ligands into potent PROTAC degraders of AR in LNCaP cells, such as compounds 11 and 16. The favorable physicochemical properties resulted in good oral bioavailability in preclinical species; however, these PROTACs were unable to degrade the important L702H mutant AR protein. Further optimization of the AR-binding moiety ultimately identified AZ'3137 (22) as a PROTAC degrader for wild-type and mutant AR, including the most common L702H mutation. AZ'3137 inhibited AR target gene expression and AR+ cell proliferation in vitro and exhibited good cross-species oral bioavailability and in vivo tumor growth inhibition in a mouse prostate cancer xenograft model. Therefore, AZ'3137 is a useful preclinical tool compound for studying the potential of AR PROTAC degraders for the treatment of prostate cancer. By degrading AR, AZ'3137 and other AR PROTACs could inhibit AR amplification or mutated forms that arise as a result of current standard of care, such as abiraterone and enzalutamide, and thus may provide a much-needed therapy for the treatment of CRPC.

Source: <https://doi.org/10.1021/acs.jmedchem.4c00269>

### Part 3

1. Drug CyberSAR combines drug design ideas and mines the active structures reported in literature and patents. Through CyberSAR, researchers can quickly and easily obtain the target structures of interest to them, so as to explore new ideas. The Androgen Receptor (Homo sapiens) is given as an example:

AR : Androgen Receptor (Homo sapiens) Mature

Structure Info

Indication

ChemSpace

Assay Data

Bioassay

SAR Doc

Target Landscape

**Name And Taxonomy**

<b>Name</b>	Androgen Receptor
<b>Synonyms</b>	<a href="#">HYSP1</a> <a href="#">Receptors, Androgen</a> <a href="#">HUMARA</a> <a href="#">Spinal And Bulbar Muscular Atrophy</a> <a href="#">Nuclear Receptor Subfamily 3 Group C Member 4</a> <a href="#">More</a> <a href="#">SMAX1</a> <a href="#">TFM</a> <a href="#">Kennedy Disease</a> <a href="#">Androgen receptor</a> <a href="#">Dihydrotestosterone Receptor</a> <a href="#">AR8</a> <a href="#">Nuclear receptor subfamily 3 group C member 4</a> <a href="#">Dihydrotestosterone receptor</a> <a href="#">AIS</a> <a href="#">雄激素受体</a> <a href="#">SBMA</a> ...
<b>Organism</b>	Homo sapiens
<b>Class</b>	<a href="#">Transcription factor</a> <a href="#">Nuclear receptor</a> <a href="#">Nuclear hormone receptor subfamily 3</a> <a href="#">Nuclear hormone receptor subfamily 3 group C</a> <a href="#">Nuclear hormone receptor subfamily 3 group C member 4</a>
<b>Type</b>	SINGLE PROTEIN
<b>Ext. Links</b>	<a href="#">GenCards</a> <a href="#">OpenTarget</a> <a href="#">UniProt</a> <a href="#">PDB</a> <a href="#">AlphaFold</a>
<b>Physiological</b>	Steroid hormone receptors are ligand-activated transcription factors that regulate eukaryotic gene expression and affect cellular proliferation and...
<b>Function</b>	<a href="#">More</a>

### 3D Structure



### Ligands

43 Results [Download](#)

<input type="checkbox"/> 4HY <span>Approved</span>  Co-crystal Targets: <a href="#">THRFB</a> <a href="#">THRA</a> <a href="#">AR</a> <a href="#">AR</a>	<input type="checkbox"/> CA4 <span>Approved</span>  Co-crystal Targets: <a href="#">AR</a>	<input type="checkbox"/> FLF <span>Approved</span>  Co-crystal Targets: <a href="#">TTR</a> <a href="#">AR</a> <a href="#">TEAD2</a> ... <a href="#">More</a>	<input type="checkbox"/> T3 <span>Approved</span>  Co-crystal Targets: <a href="#">THRA</a> <a href="#">THRFB</a> <a href="#">AR</a> ... <a href="#">More</a>	<input type="checkbox"/> TES <span>Approved</span>  Co-crystal Targets: <a href="#">AR</a> <a href="#">DIDH</a> ... <a href="#">More</a>
---	---	--	--	---

[1](#) [2](#) [3](#) [4](#) [5](#) [6](#) ... [9](#)

2. In the target interface, select the "Chemical Space" option tab and cascade the "Cluster Structure View" tab to display the literature and patents collected by the CyberSAR platform with relevant **AR**. The molecules tested for activity in related experiments are displayed in the form of "core structure clusters". The green highlighted ones are the active molecular structures with  $IC_{50} < 1000$  nM in in vitro enzyme and cell activity test experiments reported in the literature, as well as the specific experiments, experimental results and experimental sources.

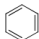
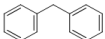
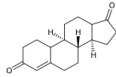
**AR : Androgen Receptor (Homo sapiens)** Mature

Structure Info | Indication | **ChemSpace** | Assay Data | Bioassay | SAR Doc

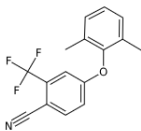
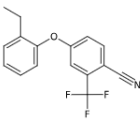
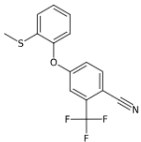
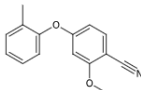
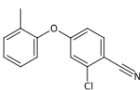
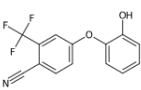
Target Landscape

Real Structure | **Cluster Structure (100)** | Clustering Threshold: **Loose** | Strict

Tips: 1- The chemical space includes molecules labeled manually and those identified through experimental data mining; 2- Manual labels are sourced from the Pharmacodia global drug database and other manually confirmed sources; Active molecules are those with activity indicators  $\leq 1000$ nM; 3- The R&D status reflects the highest development status of the molecules contained in the cluster.

<p>CC266528</p>  <p>Clustered Mol: <b>26477</b> Active Mol: <b>40</b> Clinical Mol: <b>632</b> (Approved)</p>	<p>CC331945</p>  <p>Clustered Mol: <b>2509</b> Active Mol: <b>30</b> Clinical Mol: <b>86</b> (Approved)</p>	<p>CC331807</p>  <p>Clustered Mol: <b>565</b> Active Mol: <b>17</b> Clinical Mol: <b>66</b> (Approved)</p>
--	--	--

Assay Data | **CC331945** 66 Results | Filter | Sort | Default | DES | Page Size | 10

<p>C236655 Preclinical</p>  <p><b>IC50 = 10 nM</b> Displacement of [3H]DHT from human cloned androgen receptor expressed in insect Sf9 cell system <a href="https://doi.org/10.1016/j.bmcl.2009.02.104">10.1016/j.bmcl.2009.02.104</a></p>	<p>C236613 Preclinical</p>  <p><b>IC50 = 20 nM</b> Displacement of [3H]DHT from human cloned androgen receptor expressed in insect Sf9 cell system <a href="https://doi.org/10.1016/j.bmcl.2009.02.104">10.1016/j.bmcl.2009.02.104</a></p>	<p>C236658 Preclinical</p>  <p><b>IC50 = 22 nM</b> Antagonist activity at human androgen receptor expressed in human MDA-MB-231 cells assessed as inhibition of DHT-induced response <a href="https://doi.org/10.1016/j.bmcl.2009.02.104">10.1016/j.bmcl.2009.02.104</a></p>
<p>C214748 Preclinical</p>  <p><b>IC50 = 24 nM</b> Displacement of [3H]DHT from human cloned androgen receptor expressed in Sf9 cells</p>	<p>C236535 Preclinical</p>  <p><b>IC50 = 30 nM</b> Displacement of [3H]DHT from human cloned androgen receptor expressed in insect Sf9 cell system</p>	<p>C236657 Preclinical</p>  <p><b>IC50 = 34 nM</b> Displacement of [3H]DHT from human cloned androgen receptor expressed in insect Sf9 cell system</p>

3. In the target interface, select the "Chemical Space" option tab and cascade the "Original Structure View" tab to display the literature collected by the CyberSAR platform with relevant **AR**. The molecules tested for activity in related experiments are displayed in the form of a "timeline of research and development stages". The "data mining" highlighted in green font is the potential hit.

## AR : Androgen Receptor (Homo sapiens)

Mature

Structure Info | **Real Structure (1852)** | Cluster Structure (100) | Data Range | Manual Label | Data Mining

Indication

ChemSpace

Assay Data

Bioassay

SAR Doc

Target Landscape

Tips: 1- The chemical space includes molecules labeled manually and those identified through experimental data mining; 2- The R&D status reflects the highest development status of the molecules.

**Approved (46)**  
Manual Label 36  
Data Mining 10

**Progesterone**  
Assay Data

**Estradiol transdermal**  
Assay Data

**Medroxyprogesterone...**  
Assay Data

**Salicylamide**  
Assay Data

**NDA (1)**  
Manual Label 1  
Data Mining 0

**Luxdegallutamide**  
Assay Data

**Phase 3 Clinical (7)**  
Manual Label 6  
Data Mining 1

**Asoprisnil**  
Assay Data

**Diindolylmethane**  
Assay Data

**Pyrilutamide**  
Assay Data

**Enobosarm**  
Assay Data

**Phase 2 Clinical (30)**  
Manual Label 24  
Data Mining 6

**Stanoalone**  
Assay Data

**HE-2100**  
Assay Data

**Lonaprisan**  
Assay Data

**Metribolone**  
Assay Data

**Phase 1 Clinical (12)**  
Manual Label 11  
Data Mining 1

**ORIC-101**  
Assay Data

**BMS-641988**  
Assay Data

**GLPG-0492**  
Assay Data

**Andarine**  
Assay Data

**Preclinical (1756)**  
Manual Label 38  
Data Mining 1718

**C423**  
Assay Data

**C461**  
Assay Data

**C462**  
Assay Data

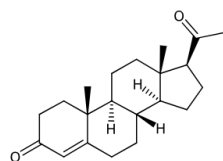
**C464**  
Assay Data

4. Clicking the "Skeleton/structure Similarity" tab can further provide derivative types of the ligand structure of Interest, which can be downloaded for further molecular evaluation or explore variation by chemist's experience

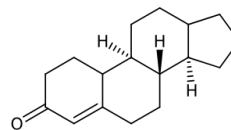
## Progesterone

- Structure Info
- Scaffold Similarity**
- Bioisosteric Expansion
- Assay Data
- Bioassay
- Indication
- SAR Doc

Pharmacodia Drug DB



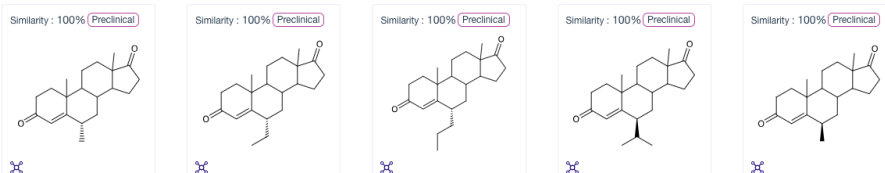
Real Structure CC(=O)[C@H]1CC[C@@H]2[C@@H]3CCC4=CC(=O)CC[C@]34[C@@H]12 Copy



Scaffold Structure O=C1C=C2CC[C@H]3[C@@H]4CCCC4CC[C@H]32 Copy

Scaffold Similarity

**Structure Similarity**



To Explore Cyber-AIDD further Login using the below Link

CyberSAR login URL on computer browser <https://cyber.pharmacodia.com/#/homePage>,  
welcome to try it out.

If you need further communication,

**For a free trial, Contact us on**

**Anil Ranadev**

+91 9742627845

[anil\\_ranadev@saspinjara.com](mailto:anil_ranadev@saspinjara.com)

**Aravind**

+91 9619076286

[aravind.p@saspinjara.com](mailto:aravind.p@saspinjara.com)

**Sachin Marihal**

+91 9538033363

[sachin.marihal@saspinjara.com](mailto:sachin.marihal@saspinjara.com)

**Chetan S**

+91 7022031061

[chetans@saspinjara.com](mailto:chetans@saspinjara.com)